ISSN 2176-5480

22nd International Congress of Mechanical Engineering (COBEM 2013)
November 3-7, 2013, Ribeirão Preto, SP, Brazil

BRAZILIAN 14-X B HYPERSONIC SCRAMJET AEROSPACE VEHICLE AEROTHERMODYNAMIC CODE

Jayme Rodrigues Teixeira da Silva
Universidade do Vale do Paraíba/UNIVAP, Campus Urbanova Av. Shishima Hifumi, nº 2911 Urbanova CEP. 12244-000 São José dos Campos, SP - Brasil
jaymerts@hotmail.com

Paulo Gilberto de Paula Toro
Instituto de Estudos Avançados/IEAv, Trevo Coronel Aviador José Alberto Albano do Amarante, nº 1 Putim CEP. 12.228-001 São José dos Campos, SP, Brasil
toro@ieav.cta.br

Abstract. *An in-house Fortran code has been developed to estimate the aerothermodynamic properties along of the streamlines at lower surfaces of the Brazilian 14-X Hypersonic Aerospace Vehicle, VHA 14-X B. The in-house Fortran code is based on the flight speeds, the frontal area of the incoming airflow and the deflection angles of the air intake of the hypersonic aerospace vehicle into the Earth's atmosphere. The air properties up to 86km geometric altitude are calculated based on the U.S. Standard Atmosphere from 1976. One-dimensional oblique shock wave and Prandtl-Meyer theories are used to determine the flow properties at the compression and expansion regions on the lower surface at the VHA 14-X B. Results of the incident and reflected shock wave as well as of the expansion wave. Static pressure, static temperature and static density as well as velocity (Mach number) of the supersonic airflow at the lower streamline of the VHA 14-X B are compared with the available results in the opened scientific literature. The in-house code drastically reduces the time and costs associated with the expensive time consuming of the Computational Fluid Dynamics commercial code as well as the high costs of the experimental investigations on hypersonic ground-based test facilities.*

Keywords*: VHA 14-X B, hypersonic airbreathing propulsion, scramjet, hypersonic shock tunnel.*

1. THE BRAZILIAN 14-X B HYPERSONIC AEROSPACE VEHICLE

The aerospace technological products have grown that one cannot conceive of putting payloads (satellites) into Earth orbit or beyond using technologies in operation (rockets carry out solid or liquid fuel). The knowledge required to keep the current launching vehicles is already so high that if the countries do not have a technological support for their own industry, they will depend on of the supplier countries and not have independent capacity sustained. Aerospace vehicle limitations for launching payloads into orbit or beyond require a continuous reduction in size, weight and power consumption of launch vehicles. Some solutions to these challenges require paradigm shifts, new production methods, and new technologies of strategic nature. The requirements of platforms launched satellites, high performance and reliability, as well as the strict limitations of fuel (reduction of size, weight and power consumption) for launching payloads into orbit or beyond provide the development of hypersonic aircraft using hypersonic airbreathing propulsion based on supersonic combustion.

The recent intensification of international efforts to develop hypersonic propulsion system based on supersonic combustion, signals that this is the way of effective access to space in a not too distant future. Therefore, the field of Hypersonic Airbreathing Propulsion based on supersonic combustion will be essential in the near future for the aerospace industry, and allow the man to build hypersonic planes, to reach other continents in hours and achieve low orbits around Earth.

The recent success to demonstrate the supersonic combustion concept, through the (about 10s burnt hydrogen scramjet-powered at Mach 7 and 10) X-43 Aerospace Vehicle flights (Moses et al., 2004; Harsha et al., 2005; Marshal et al., 2005a, 2005b) and the (about 140s burnt hydrocarbon scramjet-powered at Mach number 6+) X-51 Aerospace Vehicle flight (Hank et al., 2008) provided by the new U.S. hypersonics strategy formulated (after NASP program) by NASA, U.S. Government agencies (Air Force, Army and Navy) and DARPA for the next generation of space transportation systems under NASA Marshall Space Flight Center's Advanced Space Transportation Program (ASTP) gave a fresh renaissance in hypersonic flight.

The Brazilian VHA 14-X project, which is a hypersonic airbreathing vehicle with airframe-integrated scramjet engine, has being designed since 2007, at the Prof. Henry T. Nagamatsu Laboratory of Aerothermodynamics and Hypersonics, at the Institute for Advanced Studies (IEAv), Brazil (Ricco et al., 2011, Toro et al., 2012), to demonstrate a "scramjet" technology, in free flight, at 30km altitude at Mach number 7 to 10.

In March 2012, the coordination of the VHA 14-X proposed new versions based on the VHA 14-X (Toro et al., 2013), where the VHA 14-X B (Fig. 1) has been designed to demonstrate the scramjet technology at 30km altitude with Mach number 7, using the Brazilian solid rocket engines (S31 and S30).

ISSN 2176-5480

Analytical theoretical analysis (Galvão and Toro, 2013), computational fluid dynamics simulation (Carvalhal et al, 2013) and experimental investigation (Martos et al., 2013) are the methodology tools used to design a technological demonstrator, before flight through Earth's atmosphere.

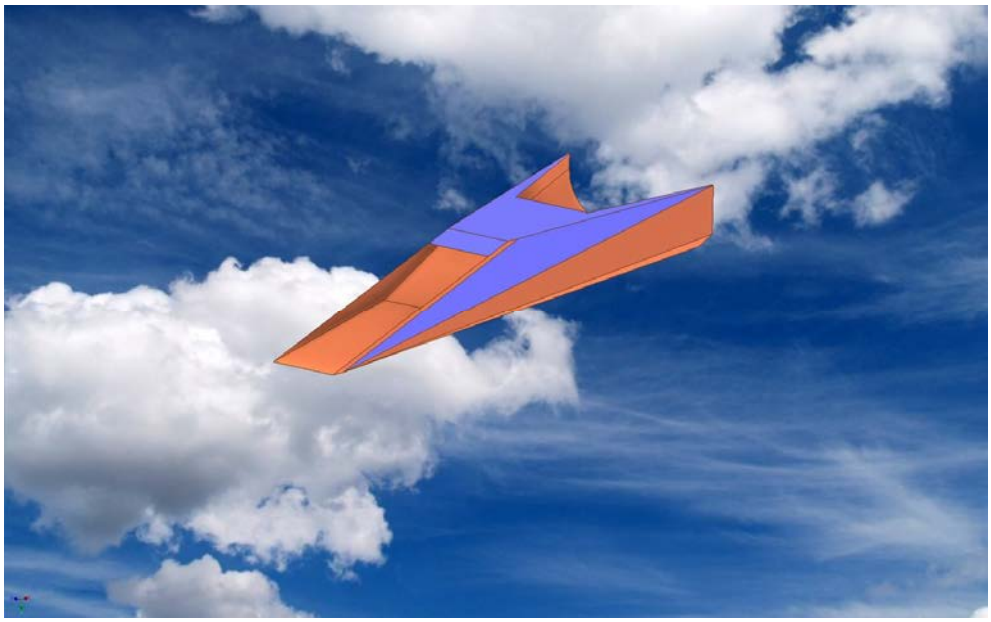

Figure 1. 14-X B Hypersonic Aerospace Vehicle, VHA 14-X B.

Basically, the scramjet is a fully integrated airbreathing aeronautical engine that uses the oblique/conical shock waves generated during the hypersonic flight, to provide compression and deceleration of freestream atmospheric air at the inlet of the scramjet. Therefore, the VHA 14-X B is operational only at hypersonic speeds, and a hypersonic accelerator vehicle will be needed to reach the VHA 14-X B at 30km altitude at Mach number 7. As a low-cost solution to launch scramjet integrated vehicle to flight test conditions (30km altitude at Mach number 7) is to use rocket engines based on solid propulsion, in ballistic trajectory. Such approach may provide an affordable path for maturing Brazilian hypersonic airbreathing components and systems in flight.

2. THEORETICAL ANALYSIS

Physical processes and flow chemistry existing in phenomena such as boundary layer transition, turbulence, viscous boundary layer/shock interactions, flow separation under adverse pressure gradient, real gas effects, radiation, ablation are still beyond the current capability of computation fluid dynamics. On top of that, numerical solutions need high quality flight-tests and/or ground-based test facilities experimental data to validate the data from the available numerical codes.

Therefore, ground-based test facilities are one of the most important methodologies for hypersonic vehicle design to be considered, although there is no single ground-based test facility capable of duplicating all hypersonic flight environments.

Facility wall temperature and power needed to run the facility as well as the high enthalpy with real gas effects are the limitations of the continuous flow ground test facilities to duplicate the environment conditions for Mach number higher than 4. High enthalpy and thermochemical characteristics of the flying vehicle in hypersonic speeds through the atmosphere are the aerothermodynamic environments that cannot be duplicated by short duration blowdown facilities.

Only impulse facilities are capable of providing enough total temperature and Mach number to duplicate the high enthalpy and thermochemical characteristics close to those encountered during the flight of vehicles at high-speeds in the Earth's atmosphere. Because of the highly transient nature of the flows involved in impulse facilities, adequate intrusive and non-intrusive very fast response time flow measurement instrumentation are necessary for successful use of these facilities, such as R & D (Research and Development) facility or T & E (Test and Evaluation) facility.

Analytical theoretical analysis provides simplified mathematical models; those are able to obtain a fast and reliable set of optimal parameters to be used on the nose-to-tail hypersonic vehicle with airframe-integrated scramjet engine preliminary design.

A nomenclature needed not only in the analytic theoretical analysis but also may be used in the numerical simulation and experimental investigations are presented by Heiser and Pratt (1994) and it is adapted for the VHA 14-X B. which it is divided in three main components (Fig. 2): external and internal compression section (inlet), combustion chamber (combustor) and internal and external expansion section (outlet).

ISSN 2176-5480

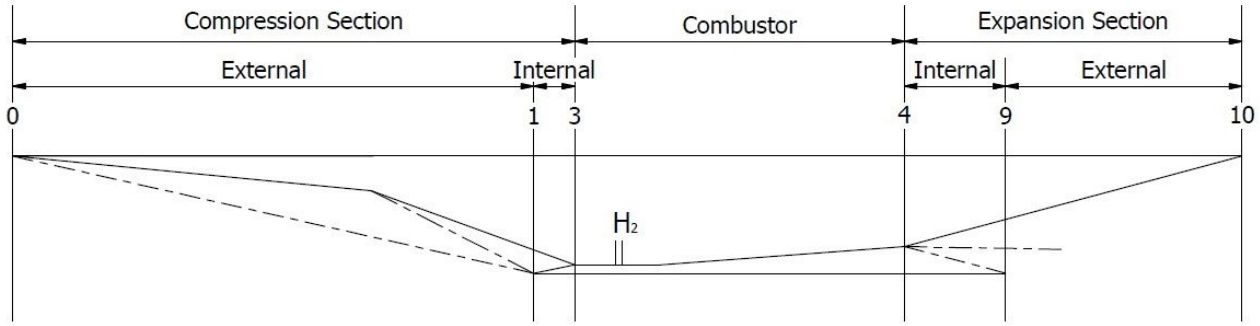

Figure 2. Hypersonic vehicle with airframe-integrated scramjet engine stations and reference terminology.

This present analytical theoretical analysis has been carried out on the VHA 14-X B (Fig. 3) framework. The VHA 14-X B consists a two-dimensional configuration (Fig. 1), with a constant cross-section (Fig. 3), where the upper flat surface, with zero angle of attack, is aligned with the freestream Mach number 7 hypersonic airflow. The lower surface, taken from the VHA 14-X waverider external configuration (Rolim, 2009; Rolim et al., 2009; Rolim et al., 2011; Costa, 2011; Costa et al., 2012, Costa et al., 2013) consists of a frontal surface with a leading edge angle of 5.5^o, compression ramp angle of 14.5^o (related to the angle of the leading edge), the internal expansion chamber combustion angle of 4.27^o and external expansion angle of 10.73^o (related to the angle of internal expansion). The cross-section height is $165-mm.$. The combustor chamber $258.63-mm.$ long with constant area, following by $134-mm.$ long with 4.27^o (to accommodate the boundary layer and expansion due H_2 and O_2 combustion) was defined by research of the Hyslop (1998) and Kasal et al. (2002), respectively. The constant area combustion chamber is $15.2-mm.$ high (to accommodate the airflow captured by the VHA 14-X B frontal area).

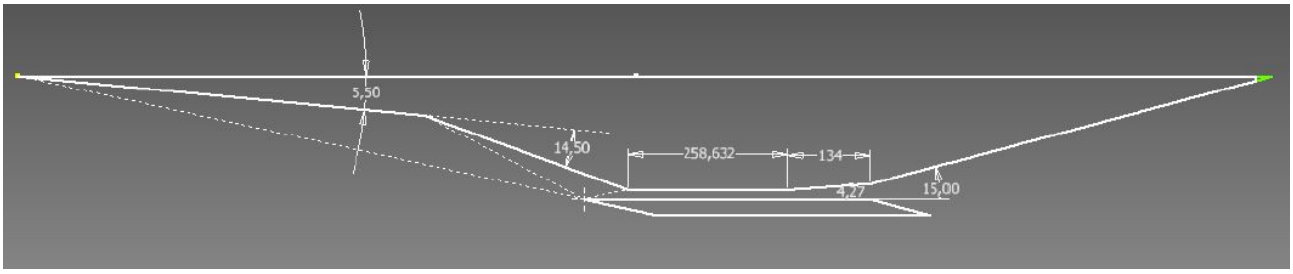

Figure 3. Cross-section of the V14-X B.

Along the present analytical theoretical analysis the subscripts *in* and *out* will be used to identify the upstream (inlet) and the downstream (outlet) conditions, respectively, at each station (Fig. 2) of the hypersonic vehicle with airframe-integrated scramjet engine lower surface.

2.1 External and Internal Compression Section (Oblique Shock Wave)

For calorically and/or thermally perfect gas ($p=\rho RT$, $\gamma=\text{constant}$) the oblique shock relationships may be easily obtained as closed form of the thermodynamic property (static pressure, static density and static temperature) ratios and Mach number across the oblique shock wave (Fig. 4) given by:

$$\frac{p_{out}}{p_{in}}=1+\frac{2\gamma}{(\gamma+1)}\left[\left(M_{in}\,sen\beta\right)^2-1\right] \tag{1}$$

$$\frac{\rho_{out}}{\rho_{in}}=\frac{(\gamma+1)\left(M_{in}\,sen\beta\right)^2}{\left[(\gamma-1)\left(M_{in}\,sen\beta\right)^2+2\right]} \tag{2}$$

$$\frac{T_{out}}{T_{in}}=\frac{p_{out}}{p_{in}}\;\frac{\rho_{in}}{\rho_{out}}=1+\frac{2\gamma}{(\gamma+1)}\left[\left(M_{in}\,sen\beta\right)^2-1\right]\frac{\left[(\gamma-1)\left(M_{in}\,sen\beta\right)^2+2\right]}{(\gamma+1)\left(M_{in}\,sen\beta\right)^2} \tag{3}$$

ISSN 2176-5480

$$M_{out} = \frac{\sqrt{\dfrac{\left(M_{in}\ sen\beta\right)^2 + \dfrac{2}{(\gamma-1)}}{\dfrac{2\gamma}{(\gamma-1)}\left(M_{in}\ sen\beta\right)^2 - 1}}}{sen\left(\beta - \theta_s\right)} \tag{4}$$

where: ρ, p, T are density, pressure, temperature of the gas, respectively; u is the velocity across the oblique shock wave; θ_s and β are the deflection and shock wave angles, respectively. Additionally, the shock wave angle β with respect to the local flow direction θ_s may be obtained iteratively with the relationship given by:

$$tg\theta_s = 2\left(\text{cotg}\ \beta\right)\left[\frac{\left(M_{in}\ sen\beta\right)^2 - 1}{M_{in}^2\left(\gamma + \cos 2\beta\right) + 2}\right] \tag{5}$$

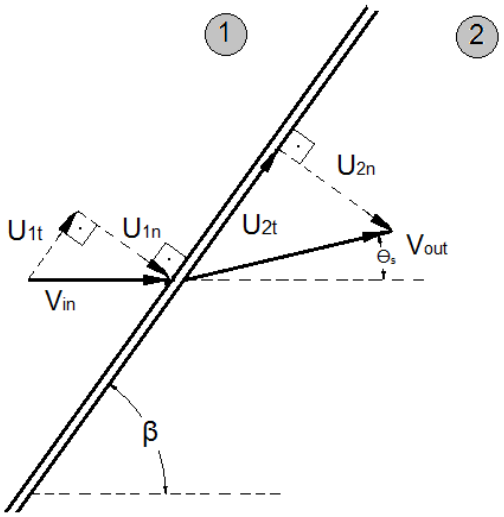

Figure 4. Incident Oblique Shock wave geometry.

Note the flow across the oblique shock wave promote an increase of pressure, density, temperature, and a decrease of Mach number, however the flow remains supersonic/hypersonic and parallel to the flat surface of the external and internal compression section (Fig. 3) of the hypersonic vehicle with airframe-integrated scramjet engine lower surface.

2.2 Combustor Section (One-Dimensional Flow with Heat Addition)

The one-dimensional with constant-area heat addition, Rayleigh Flow, (Fig. 5) may be applied to combustion processes between the entrance (inlet) and the exit (outlet) of the scramjet combustor (Fig. 3), where the combustion processes correspond to heat addition at constant pressure, constant density, constant temperature and constant Mach number, respectively, at the inlet of the scramjet combustor. The one-dimensional with constant-area heat addition (Anderson, 2003) are given by:

$$\rho_{in}\ u_{in} = \rho_{out}\ u_{out} \tag{6}$$

$$p_{in} + \rho_{in}\ u_{in}^2 = p_{out} + \rho_{out}\ u_{out}^2 \tag{7}$$

$$h_{in} + \frac{u_{in}^2}{2} + q = h_{out} + \frac{u_{out}^2}{2} \tag{8}$$

ISSN 2176-5480

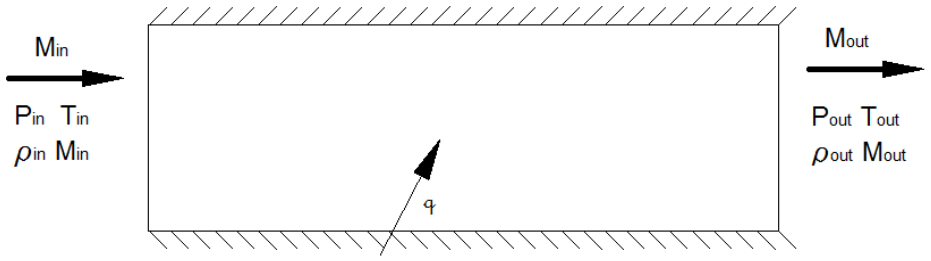

Figure 5. Rayleigh Flow, one-dimensional with constant-area heat addition.

The energy equation (Eq. 8) indicates the heat addition change the total energy (temperature). For calorically and/or thermally perfect gas ($p = \rho RT$, $\gamma = \text{constant}$) and applying the total temperature definition, obtain

$$q = c_p \left(T_{o,\,out} - T_{o,\,in} \right) \tag{9}$$

where: the total temperature is given by:

$$\frac{T_o}{T} = 1 + \frac{\gamma - 1}{2} M^2 \tag{10}$$

Closed form of the thermodynamic property (pressure, density and temperature) ratios across constant-area heat addition may be obtained by manipulating the x-direction momentum equation, and they are given by:

$$\frac{p_{out}}{p_{in}} = \left(\frac{1 + \gamma\, M_{in}^2}{1 + \gamma\, M_{out}^2} \right) \tag{11}$$

$$\frac{T_{out}}{T_{in}} = \left(\frac{1 + \gamma\, M_{in}^2}{1 + \gamma\, M_{out}^2} \right)^2 \left(\frac{M_{out}^2}{M_{in}^2} \right)^2 \tag{12}$$

$$\frac{\rho_{out}}{\rho_{in}} = \left(\frac{1 + \gamma\, M_{out}^2}{1 + \gamma\, M_{in}^2} \right) \left(\frac{M_{in}^2}{M_{out}^2} \right)^2 \tag{13}$$

Note the flow from the external and internal compression section are deflected to the combustor entrance (Fig. 3) at supersonic speed (at constant pressure, constant density, constant temperature and constant Mach number). Fuel (H_2) will be injected right after the entrance station (Fig. 3) in (minimal) sonic speed. Rayleigh flow (one-dimensional flow with heat addition) may be applied to the combustion process between H_2 and O_2 burning in supersonic speed, resulting at the exit of the combustor chamber (outlet) an increase in pressure, density, temperature, reducing the Mach number.

2.3 Internal and External Expansion Section (Expansion Wave)

The Prandtl-Meyer theory may be applied to the (internal and external expansion section, Fig. 3) expansion waves (Fig. 6). An isentropic expansion wave is limited by the head and tail of the expansion wave defined by the Mach angle μ_{head} , μ_{tail} , respectively, and they are given by:

$$\mu_{head} = \text{arcsen} \left(\frac{1}{M_{in}} \right) \tag{14}$$

$$\mu_{tail} = \text{arcsen} \left(\frac{1}{M_{out}} \right) \tag{15}$$

ISSN 2176-5480

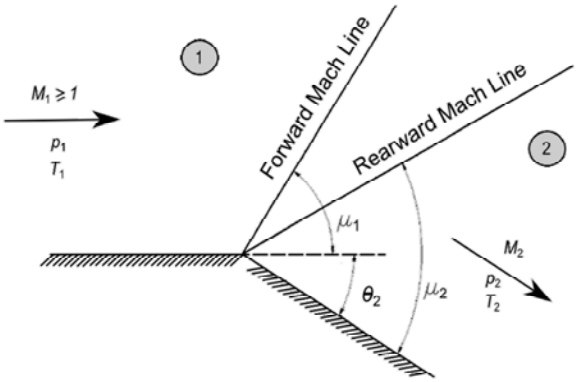

Figure 6. Expansion wave geometry.

The expansion deflection angle θ_e is given by the Prandtl-Meyer function $\upsilon(\mathrm{M})$:

$$\theta_e = \upsilon\left(M_{out}\right) - \upsilon\left(M_{in}\right) \tag{16}$$

where: The Prandtl-Meyer function $\upsilon(\mathrm{M})$, which is function of the Mach number, is given by:

$$\upsilon(M) = \sqrt{\frac{\gamma+1}{\gamma-1}}\ tg^{-1}\sqrt{\frac{\gamma-1}{\gamma+1}\left[M^2-1\right]} - tg^{-1}\sqrt{M^2-1} \tag{17}$$

Once Mach number after expansion wave $\mathrm{M}_{\mathrm{out}}$ is determined the closed form of the thermodynamic property (pressure, density and temperature) ratios across the expansion wave may be obtained by the isentropic relationships given by:

$$\frac{T_{out}}{T_{in}} = \left(\frac{1+\frac{\gamma-1}{2}M_{in}^2}{1+\frac{\gamma-1}{2}M_{out}^2}\right) \tag{18}$$

$$\frac{p_{out}}{p_{in}} = \left(\frac{T_{out}}{T_{in}}\right)^{\frac{\gamma}{\gamma-1}} \tag{19}$$

$$\frac{\rho_{out}}{\rho_{in}} = \frac{p_{out}}{p_{in}}\frac{T_{in}}{T_{out}} \tag{20}$$

Note the flow across the expansion wave promote a decrease of pressure, density, temperature, and an increase of Mach number. The flow remains supersonic/hypersonic and parallel to the flat surface of the internal and external expansion section (Fig. 3) of the hypersonic vehicle with airframe-integrated scramjet engine lower surface.

3. THE EARTH'S ATMOSPHERIC THERMODYNAMIC PROPERTIES

Any hypersonic airbreathing propulsion interacts with the Earth's atmosphere and it is necessary to understand the environment and to quantify the Earth's thermodynamic properties.

Hypersonic vehicle with airframe-integrated scramjet engine is designed to fly thought the Earth's atmosphere up to altitude of 70km due to mass flux necessary to burn the Hydrogen at the combustor.

The static pressure, static temperature and static density as well as the chemical constituents of the Earth's mixture of nitrogen and oxygen atmosphere change continuously primarily due to solar influence. Atmospheric air thermodynamic properties may be obtain as an averaged of "hot day" and "cold day" as function of altitude, latitude, longitude, season of the year, time the day and solar activities. Standard atmospheres have been providing from many sources, and the most useful standard atmosphere is provided by the work developed by three U. S. Agencies: National

ISSN 2176-5480

Oceanic and Atmospheric Administration, National Aeronautics and Space Administration and United States Air Force (U.S. Standard Atmosphere, 1976).

The Earth's atmosphere may be defined by several layers (Table 1) and closed relationships can be found for each of these layers. U.S. Standard Atmosphere (1976) provides closed relationships to determine the thermodynamic air properties.

Traditionally, standard atmospheres have defined temperature as a linear function of height (geometric altitude) to eliminate the need for numerical integration in the computation of pressure function of height (U.S. Standard Atmosphere, 1976), which may be related to the molecular temperature by

$$T_M = \frac{M_0}{M} T \tag{21}$$

where, M is the mean molecular weight of the air at the desire geometric altitude and M_o (28.9644 kg/kmol) is the molecular weight at the sea-level value.

The molecular temperature is a linear function of geopotential altitude H given by

$$T_M = T_{M,b} + L_{M,b}\left(H - H_b\right) \tag{22}$$

where: $L_{M,b}$ is a molecular-scale temperature gradient, $T_{M,b}$ is a geopotential temperature for each geopotential height H_b (Table 1).

Table 1. U.S. standard atmosphere temperature-altitude definitions

Layer	Geopotential height	Molecular-scale temperature gradient	Geopotential temperature	Form of function relating T_M to H	Geopotential pressure
subscript b	H_b (km´)	$L_{M,b}$ (K/km´)	$T_{M,b}$ (K)		p_b (K)
0	0	-6.5	288.15	Linear	101325.0
1	11	0	216.65	Isothermal	22632.04
2	20	+1.0	216.65	Linear	5474.875
3	32	+2.8	228.65	Linear	868.0153
4	47	0.0	270.65	Isothermal	110.9057
5	51	-2.8	270.65	Linear	66.93847
6	71	-2.0	214.65	Linear	3.956387
7	84.8520		186.87		0.3733767

The geopotential altitude is related to the geometric altitude by the Earth's radius r_o , given by

$$H = \frac{r_0 \; Z}{r_0 + Z} \frac{g}{g_o^{'}} \tag{23}$$

where $\frac{g}{g_o^{'}}$ =1m'/m

Note that the mean molecular weight of the air up to 80km geometric altitude is exactly (U.S. Standard Atmosphere, 1976) the molecular weight at the sea-level value M_o (28.9644 kg/kmol), therefore the static temperature at geometric altitude is the same as the molecular temperature at given altitude (Eq. 23).

There are two closed relations to calculate the static pressure and both are functions of molecular temperatures (geopotential altitudes). However, up to 80km (M = M_o (28.9644 kg/kmol) the static pressure at geometric altitude may be calculated directly from the molecular temperatures, which it is function of geopotential altitudes.

$$p = p_b \left[\frac{T_{m,b}}{T_{M,b} + L_{M,b}\left(H - H_b\right)} \right]^{\frac{g_o^{'} M_o}{R^* L_{M,b}}} \tag{24}$$

ISSN 2176-5480

$$p = p_b \; e^{\frac{-g_o' M_o \left(H - H_b\right)}{R^* T_{M,b}}} \tag{25}$$

where: p_b (Table 1) is the molecular pressure at desired geopotential altitude and R^* is 8314.32 (N m/kmol K). Static mass density can be calculated by the calorically perfect relation $p = \rho R T$ and sound velocity by $a = \sqrt{\gamma R T}$.

4. MODEL VALIDATION

4.1 The Earth's Atmospheric Thermodynamic Properties validation up to 86km geometric altitude

First, a Fortran code was built with the closed relationships (Eqs. 21-25) provided by the U.S. Standard Atmosphere (1976).

After, the thermodynamic air properties, temperature (Fig. 7), pressure (Fig. 8) and density (Fig. 9), were obtained up to 86km geometric altitude in tabular form and compared with the thermodynamic air property values provide (in tabular form) by the U.S. Standard Atmosphere (1976).

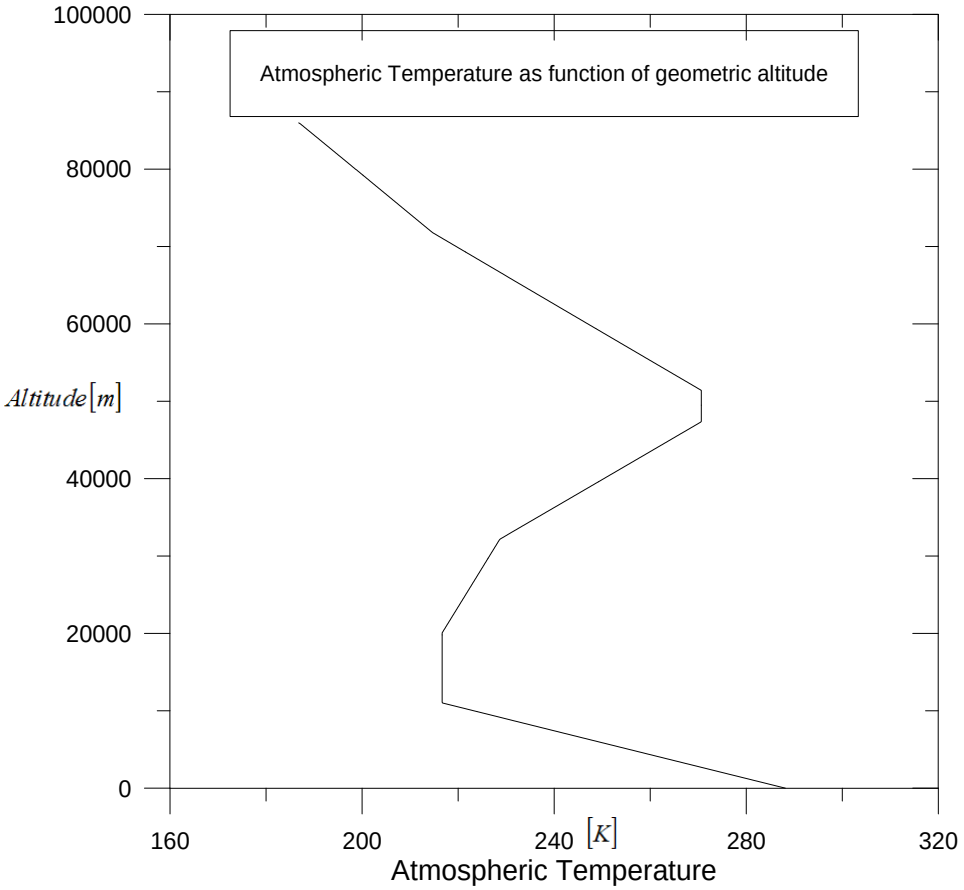

Figure 7. Static Temperature as function of geometric altitude.

ISSN 2176-5480

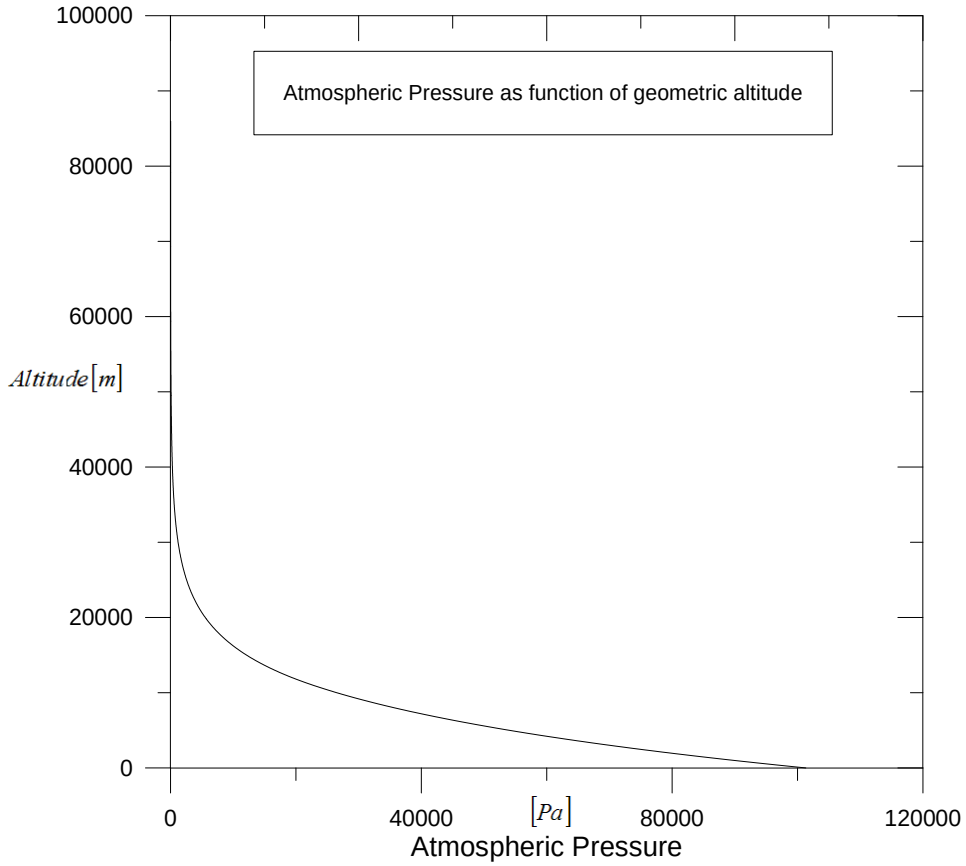

Figure 8. Static Pressure as function of geometric altitude.

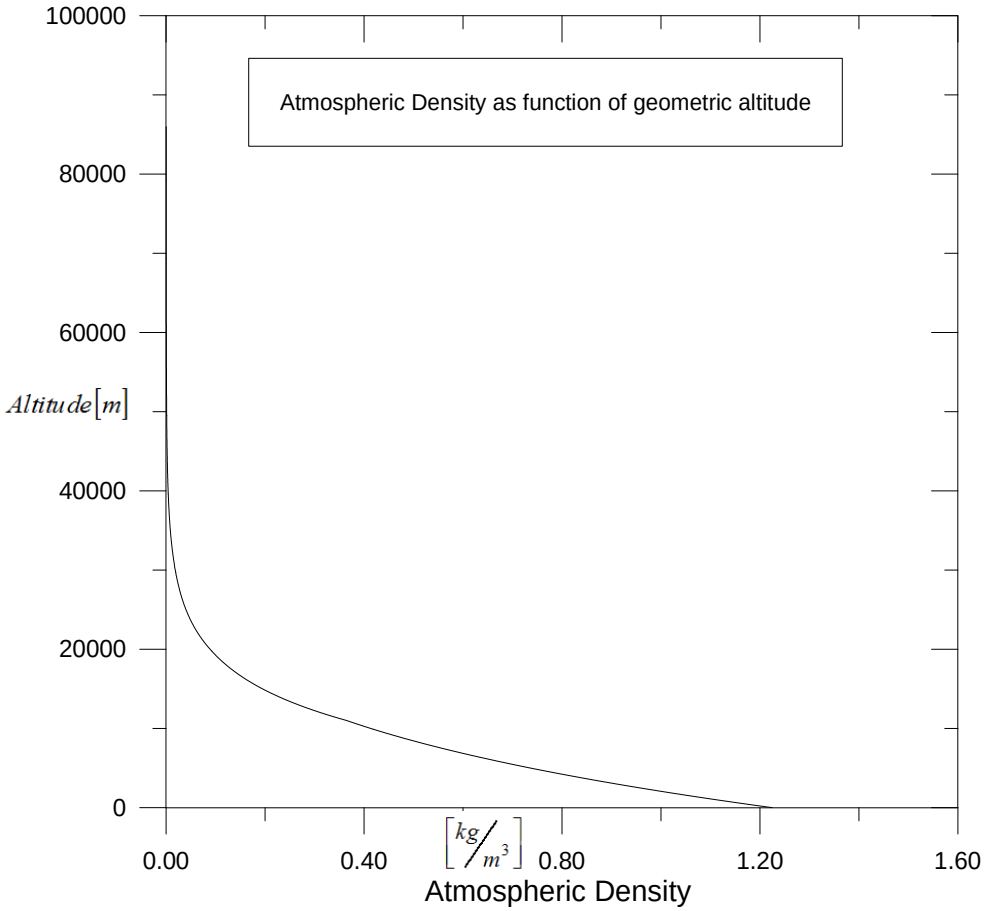

Figure 9. Static density as function of geometric altitude.

ISSN 2176-5480

4.2 Oblique Shock Wave validation

A second Fortran Code was developed to determine the thermodynamic (temperature, pressure and density) air property ratios (Eqs. 1-3), the Mach number behind the oblique shock wave (Eq. 4) and the shock wave angle (Eq. 5).

Figure 10 shows the oblique shock wave for a given deflection wedge angle (Fig. 4), which was compared with the oblique shock wave angle presented by Anderson (2003).

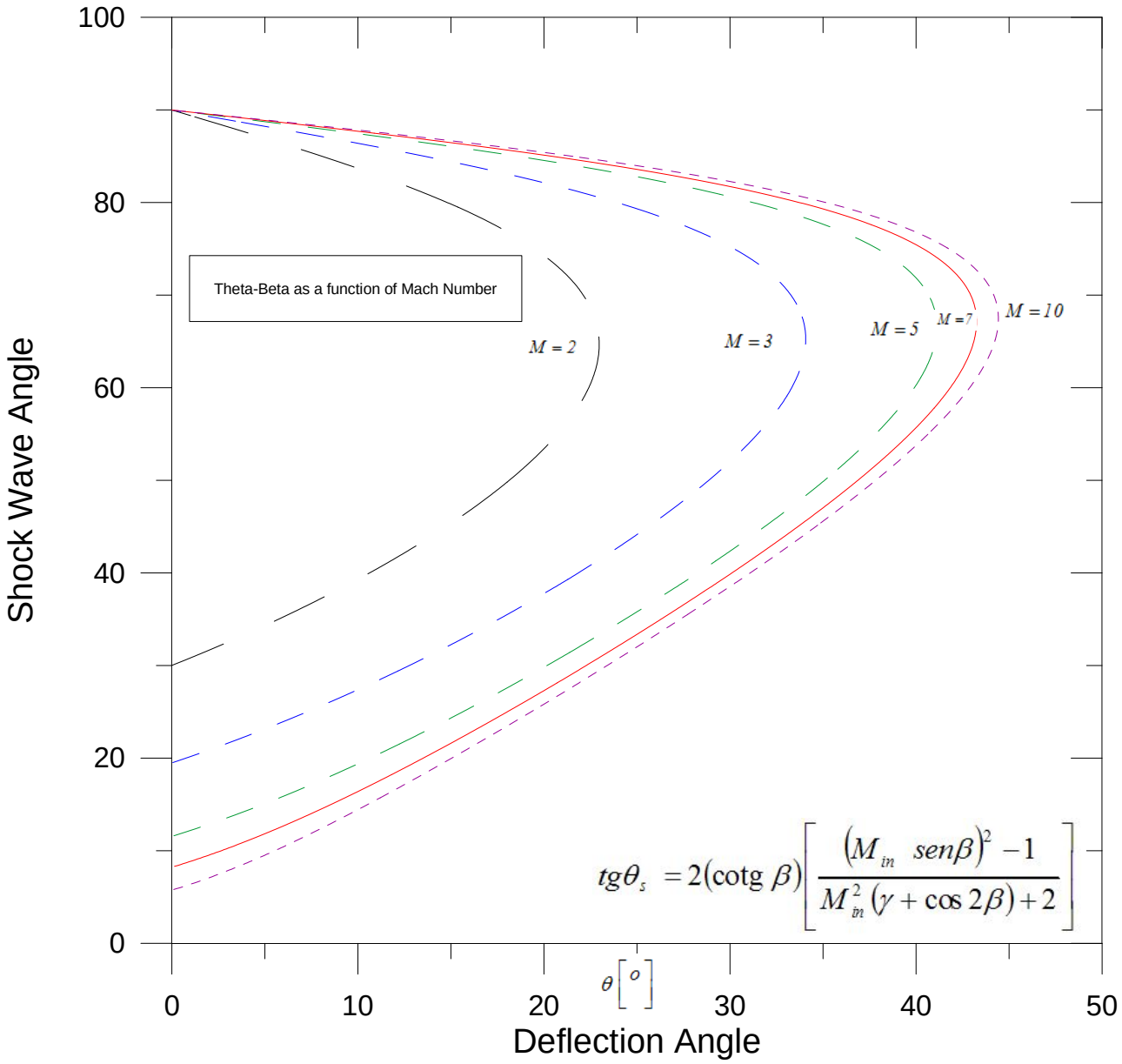

Figure 10. Oblique shock wave angle as function of freestream Mach number.

Also, the thermodynamic property ratios across the oblique shock wave were validate with the thermodynamic property ratio across the normal shock wave considering the $M_{in}^{\text{normal component of the freestream velocity}} = M_{in}\ sen\beta$ as indicates at the Fig. 4 (Anderson, 2003).

4.3 Expansion Wave validation

A third Fortran Code was developed to determine the Mach angle (Eq. 14 or Eq. 15), the Prandt-Meyer function (Eq. 17) as function of the Mach number. The results of the present third code were validated with the results presented by Anderson (2003).

Following the thermodynamic (temperature, pressure and density) air property ratios (Eqs. 18-20) were implemented at the third code and the results were validated by the results presented by Anderson (2003).

ISSN 2176-5480

4.4 First version of the Aerothermodynamic Fortran Code

The first version of the Aerothermodynamic Fortran Code was developed considering: only the calculations of the Earth's atmospheric thermodynamic properties up to 86km geometric altitude, the oblique shock wave thermodynamic property ratios and the expansion wave thermodynamic property ratios.

5. VHA 14-X B MODEL DESIGN

The Aerothermodynamic Fortran Code has been applied to evaluated the thermodynamic properties at the lower surface (Table 2) of the two-dimensional configuration of the VHA 14-X B (Fig. 3) using the reference terminology (Fig. 2), flying at 30km geometric altitude at Mach number 7.

Table 2. Thermodynamic properties at the VHA 14-X B model lower surfaces, power off, inviscid, $\gamma = 1.4$.

		station 0	station 1 (deflection 5.5º)	station 2 (deflection 14.5º)	station 3 (deflection 20º)	station 4 (Power off) (deflection 4.27º)	station 4 (deflection 10.73º)
M_{in}		7	7	6.0188	4.0645	2.6012	2.7981
θ_{in}	º		5.5	14.5	20	4.27	10.73
β_{out}	º		12.2429	22.1143	32.2384		
M_{out}			6.0188	4.0645	2.6012	2.7981	3.3715
T_{out}	K	226.5	296.6924	568.3735	1039.555	953.2721	747.1747
p_{out}	Pa	1197	2877.588	16755.91	89104.56	65803.72	28052.13
ρ_{out}	kg/m^3	0.01841	0.033788	0.102702	0.298605	0.240467	0.13079
a_{out}	m/s	301.7	345.9846	478.8732	647.6307	620.1719	549.0535
u_{out}	m/s	2111.9	2082.412	1946.38	1684.617	1735.303	1851.134
μ_{head}	º					22.6107	20.9405
μ_{tail}	º					20.9394	17.2536

6. CONCLUSION

An in-house Fortran code has been developed to estimate the aerothermodynamic properties along of the streamlines at lower surfaces of the VHA 14-X B. The in-house Fortran code is based on the flight speeds, the frontal area of the incoming airflow and the deflection angles of the air intake of the hypersonic aerospace vehicle into the Earth's atmosphere.

The in-house code drastically reduces the time and costs associated with the expensive time consuming of the Computational Fluid Dynamics commercial code as well as the high costs of the experimental investigations on hypersonic ground-based test facilities.

The Brazilian VHA 14-X B, designed at the Prof. Henry T. Nagamatsu Laboratory of Aerothermodynamics and Hypersonics, is part of the continuing effort of the Department of Aerospace Science and Technology (DCTA), to develop a technologic demonstrator using "scramjet" technology to provide hypersonic airbreathing propulsion system based on supersonic combustion.

7. ACKNOWLEDGEMENTS

The second author would like to express gratitude to FINEP (agreement nº 01.08.0365.00, project nº 0445/07) for the financial support for the 14-X Hypersonic Aerospace Vehicle design and experimental investigations; and to CNPq (project nº 520017/2009-9) for the financial support to undergraduate students.

Also, the first author acknowledges the CNPq (grant # 182135/2011-0) for financial support to undergraduate student.

ISSN 2176-5480

8. REFERENCES

Anderson Jr., J. A., 2003 "*Modern Compressible Flow, The Historical Perspective*" McGraw-Hill, Inc.

Carvalhal, A. K., Toro, P. G. P., Costa, F. J., Camillo, G. P. 2013 "Numerical Analysis of Brazilian 14-X B hypersonic aerospace vehicle at Mach number 7", internal report.

Costa, F.J. 2011 "Projeto Dimensional para Manufatura do Veículo Hipersônico Aeroespacial 14-X" (in Portuguese). UndergraduateWork, FATEC de São José dos Campos: Professor Jessen Vidal, Brazil.

Costa, F.J., Toro, P.G.P., Rolim. T.C., Camilo, G.C., Follador, R.C. and Minucci, M.A.S., 2012 "Design of the Brazilian Hypersonic waverider Aerospace Vehicle", 14th Brazilian Congress of Thermal Sciences and Engineering, October 18-22, Rio de Janeiro, RJ, Brazil

Galvão, V. A. B., Toro, P. G. P. 2013 "Analytic Theoretical Analysis of scramjet hypersonic aerospace vehicle at Mach number 7", to be presented at the 22nd Brazilian Congress of Mechanical Engineering, November 3-7, 2013, Ribeirão Preto, SP, Brazil.

Martos, J. F. A., Toro, P. G. P., Romanelli Pinto, D., Marcos, T., V. C., Camillo, G. P. , Galvão, V. A. B., Silva, C., Rêgo 2013 "Experimental Investigation of the VHA 14-X B unpowered scramjet Mach number 7", internal report.

Hank, J. M., Murphy, J. S. E Mutzman, R. C. 2018 "The X-51a Scramjet Engine Flight Demonstration Program". In: 15th Aiaa International Space Planes And Hypersonic Systems And Technologies Conference, 2008 (AIAA 2008-2540), Dayton, Ohio, EUA.

Harsha, P. T., Keel, L. C., Castrogiovanni, E. A. E Sherrill, R. T. 2005 a "X-43a Vehicle Design And Manufacture". In: Aiaa/Cira 13th International Space Planes And Hypersonic Systems And Technologies Conference, (AIAA 2005-3334), Capua, Italia.

Heiser, H. W. E Pratt, D. T (Com Daley, D. H. E Mehta, U. B.), 1994. *Hypersonic Airbreathing Propulsion.* Education Series. Eua. AIAA.

Hyslop, P. 1998 CFD Modelling Of Supersonic Combustion In A Scramjet Engine. Tese (Doutorado Em Engenharia Aeronáutica) – The Australian National University.

Kasal, P, Gerlinger, P., Walther, R., Wolfersdorf, J. V. and Weigand, B. 2002 "Supersonic Combustion: Fundamental Investigations of Aerothermodynamic Key Problems". AIAA-2002-5119.

Marshall, L. A., Corpening, G. P. E Sherrill, R. A., 2005a Chief Engineer's View Of The Nasa X-43a Scramjet Flight Test. In: Aiaa/Cira 13th International Space Planes And Hypersonic Systems And Technologies Conference, 2005 (AIAA 2005-3332), Capua, Italia.

Marshall, L. A., Bahm, C., Corpening, G. P. E Sherrill, R. 2005 b Overview With Results And Lessons Learned Of The X-43a Mach 10 Flight. In: Aiaa/Cira 13th International Space Planes And Hypersonic Systems And Technologies Conference, 2005 (Aiaa 2005-3336), Capua, Italia.

Moses, P. L., Rausch, V. L., Nguyen, L.T. E Hill, J. R. 2004. Nasa Hypersonic Flight Demonstrators – Overview, Status, And Future Plans. **Acta Astronautica,** Vol. 55, P. 619-630.

Ricco, M.F.F., Funari, P.P., Carvalho, A.V., 2011, Espaço, Tecnologia, Ambiente E Sociedade (In Portuguese), 1st Ed., Habilis Editora Erechim, RS, Brazil, Chapter 8, 161.

Rolim, T. C. A. Experimental Analysis Of A Hypersonic Waverider. 2009. 120f. Tese (Mestrado Em Ciência, Engenharia Mecânica E Aeronáutica) – Instituto Tecnológico De Aeronáutica, São José Dos Campos, 2009.

Rolim, T. C., Minucci, M. A. S., Toro, P. G. P. and Soviero, P. A. O., 2009 "Experimental Results of a Mach 10 Conical-Flow Derived Waverider". 16th AIAA/DLR/DGLR International Space Planes and Hypersonic Systems and Technologies Conference.AIAA 2009-7433.

Rolim, T.C., Toro, P.G.P., Minucci, M.A.S, Oliveira, A.C. and Follador, R.C., 2011, "Experimental results of a Mach 10 conical-flow derived waverider to 14-X hypersonic aerospace vehicle". Journal of Aerospace Technology and Management, São José dos Campos, Vol.3, No.2, pp. 127-136, May-Aug..

Toro, P. G. P., Minucci, M. A. S., Rolim, T. C., Follador, R. C., Santos, A. M., Camillo, G. P., Barreta, L. G.. 2012 "Brazilian 14-X Hypersonic Aerospace Vehicle Project". 18th AIAA International Space Planes and Hypersonic Systems and Technologies Conference, 22-28 Set,Tours, France.

U.S. Standard Atmosphere, 1976. NASA TM-X 74335. National Oceanic and Atmospheric Administration, National Aeronautics and Space Administration and United States Air Force.

9. RESPONSIBILITY NOTICE

The authors are the only responsible for the printed material included in this paper.